Large, stratified, and mechanically functional human cartilage grown in vitro by mesenchymal condensation

Sarindr Bhumiratana[a], Ryan E. Eton[a], Sevan R. Oungoulian[b], Leo Q. Wan[c], Gerard A. Ateshian[b], and Gordana Vunjak-Novakovic[a,1]

[a]Department of Biomedical Engineering, Columbia University, New York, NY 10032; [b]Department of Mechanical Engineering, Columbia University, New York, NY 10027; and [c]Department of Biomedical Engineering, Rensselaer Polytechnic Institute, Troy, NY 12180

Edited* by Robert Langer, Massachusetts Institute of Technology, Cambridge, MA, and approved March 31, 2014 (received for review December 30, 2013)

The efforts to grow mechanically functional cartilage from human mesenchymal stem cells have not been successful. We report that clinically sized pieces of human cartilage with physiologic stratification and biomechanics can be grown in vitro by recapitulating some aspects of the developmental process of mesenchymal condensation. By exposure to transforming growth factor-β, mesenchymal stem cells were induced to condense into cellular bodies, undergo chondrogenic differentiation, and form cartilagenous tissue, in a process designed to mimic mesenchymal condensation leading into chondrogenesis. We discovered that the condensed mesenchymal cell bodies (CMBs) formed in vitro set an outer boundary after 5 d of culture, as indicated by the expression of mesenchymal condensation genes and deposition of tenascin. Before setting of boundaries, the CMBs could be fused into homogenous cellular aggregates giving rise to well-differentiated and mechanically functional cartilage. We used the mesenchymal condensation and fusion of CMBs to grow centimeter-sized, anatomically shaped pieces of human articular cartilage over 5 wk of culture. For the first time to our knowledge biomechanical properties of cartilage derived from human mesenchymal cells were comparable to native cartilage, with the Young's modulus of >800 kPa and equilibrium friction coeffcient of <0.3. We also demonstrate that CMBs have capability to form mechanically strong cartilage–cartilage interface in an in vitro cartilage defect model. The CMBs, which acted as "lego-like" blocks of neocartilage, were capable of assembling into human cartilage with physiologic-like structure and mechanical properties.

tissue engineering | biomimetic | regenerative medicine | cartilage repair | cartilage mechanics

Generation of functional tissues in vitro from a patient's cells would revolutionize regenerative medicine, by providing biological substitutes for the tissues lost or damaged due to injury, disease, or aging (1, 2). Our growing understanding of the embryonic development and stem cell biology has greatly influenced the tissue engineering approaches to scaffold design, cell manipulation, and incorporation of factors (biochemical and physical) that regulate stem cell differentiation and tissue formation.

Tissue engineering is of particular interest to cartilage regeneration, as cartilage exhibits only minimal capability for intrinsic healing due to its avascular nature (3). The hallmark characteristics of cartilage disease include the loss of mechanical properties, collagen degradation, reduced proteoglycan synthesis, and decreased cellularity (4, 5). Approaches to the repair of focal cartilage lesions include laser solder welding (6), autograft cell/tissue transfer via periosteal grafts (7), mosaicplasty (8), and the autologous chondrocyte implantation method for cartilage regeneration (9). Whereas these options offer a temporary relief of symptoms, they also introduce long-term problems. There is a major ongoing effort to develop cell-based therapies for regenerating functional cartilage tissue (10–13).

In cartilage tissue engineering, scaffolding materials have been successfully used with primary bovine chondrocytes to engineer cartilage with properties approximating those of native tissue (14, 15). Notably, such result has not been achieved to date using human mesenchymal stem cells (hMSCs)— the most attractive cell source for clinical application (16). The methods that were successful with primary chondrocytes resulted in subnormal cartilaginous tissues when used with mesenchymal cells (16). We hypothesized that the lack of success was due to some critical signals for cell differentiation and early cartilage development missing from the cell milieu.

To test this hypothesis, we designed a cellular self-assembly method (14, 17, 18) that mimics mesenchymal condensation, a pivotal stage in the development of skeletal and other mesenchymal tissues that is mediated by cell adhesion molecules and extracellular matrix (ECM) (19). During physiologic condensation, cells form dense cellular bodies that undergo a series of mesenchymal condensation stages (19, 20). Early on, mesenchymal condensation sets boundaries that define the subsequent growth and differentiation of cellular bodies (21, 22). In vitro, mesenchymal stem cells were shown to undergo cellular condensation and chondrogenesis in the presence of regulatory factors such as TGF-β (23, 24). Despite the critical role of mesenchymal condensation in physiologic development, this process has not been implemented in engineering of skeletal tissues.

We investigated the mesenchymal stem cell condensation as a method to engineer functional human cartilage. We first studied the developmental stages of cellular condensation and boundary setting, and showed that condensed mesenchymal cell bodies (CMBs) can be induced to form large homogenous cell aggregates by fusing before the setting of their condensation boundaries. This method was used to generate centimeter-sized, anatomically shaped articular cartilage constructs with

Significance

The ability to regenerate functional cartilage from adult human mesenchymal stem cells would have tremendous clinical impact. Despite significant efforts, mechanically functional human cartilage has not been grown in vitro. We report engineering of functional human cartilage from mesenchymal stem cells, by mimicking the physiologic developmental process of mesenchymal cell condensation. Condensed mesenchymal bodies were induced to fuse and form mechanically functional cartilaginous tissue interfacing with bone, without using a scaffolding material. We demonstrate that this simple "biomimetic" approach can be used to generate centimeter-sized, anatomically shaped pieces of human cartilage with physiologic stratification and mechanical properties. Functional human cartilage grown from a patient's own cells using this method could greatly accelerate the development of new therapeutic modalities for cartilage repair.

Author contributions: S.B. and G.V.-N. designed research; S.B., R.E.E., and S.R.O. performed research; S.B., R.E.E., S.R.O., L.Q.W., G.A.A., and G.V.-N. analyzed data; and S.B. and G.V.-N. wrote the paper.

The authors declare no conflict of interest.

*This Direct Submission article had a prearranged editor.

[1]To whom correspondence should be addressed. E-mail: gv2131@columbia.edu.

This article contains supporting information online at www.pnas.org/lookup/suppl/doi:10.1073/pnas.1324050111/-/DCSupplemental.

physiologic stratification, stiffness, and tribological properties. Finally, the ability of CMBs to repair cartilage was shown in an in vitro cartilage-defect model. We expect that this simple and effective approach can be used as a platform for regenerative medicine not only in the context of cartilage, but also for other tissues originating from mesenchymal condensation.

Results

Optimal Size of CMBs. hMSCs were suspended in medium supplemented with TGF-β_3 and allowed to aggregate at the bottom of a well, condensed into a single cellular body after 12 h of incubation. By day 3, small aggregates (containing 1–2.5 $\times$ 10^5 cells) formed dense spherical cellular bodies in contrast to the larger aggregates (containing 5 $\times$ 10^5 to 2 $\times$ 10^6 cells) that formed biconcave disk structures indicative of inadequate condensation (Fig. 1*A*). The relative increase in the cellularity was also higher for the small than for the large aggregates (Fig. 1*B*). Therefore, we selected 2.5 $\times$ 10^5 cells for the formation of CMBs.

Boundary Setting in CMBs. After aggregation, CMBs developed and maintained their spherical structures over prolonged periods of time. To investigate the formation of tissue boundaries, we examined the production and localization of tenascin, which is a boundary-setting protein in mesenchymal condensation. The production of tenascin increased over time, such that by day 7 of condensation, a tenascin-rich ECM was present on the entire outer surface of the CMB, setting a boundary for advanced stages of condensation (Fig. 1*D*). The expression of fibronectin (*FN1*) remained stable, whereas the expression of chondrogenic differentiation factor sex determining region Y (SRY)-box 9 (*SOX9*), transcription factor for cell adhesion homeobox A2 (*HOXA2*), cell adhesion cadherin 2 (*CDH2*) gene, and boundary setting proteins tenascin C (*TNC*) and syndecan 3 (*SDC3*) all increased with time (Fig. 1*E* and Table S1), providing evidence for maturation of the condensation process and setting of the mesenchymal condensation boundaries.

Fusion of CMBs. Because CMBs develop a boundary within 7–9 d of culture, we investigated their ability to homogenously fuse with one another at various developmental stages (Fig. 1*C*). At 7 d postfusion, tenascin was present at the outer surfaces of CMBs and between adjacent CMBs, suggesting insufficient integration (Fig. 1*F*). The set boundary around maturing CMBs (7–9 d) resulted in a well-established border around tissue bodies that was maintained over 5 wk of chondrogenic differentiation (Fig. 1*F*). In contrast, homogenous integration was achieved when early stage CMBs (1–5 d of condensation) were fused together (Fig. 1*F*).

Functional Cartilage Generated from Fused CMBs. By pressing a layer of CMBs onto porous decellularized bone matrix, we generated a dense cellular region (a precursor of articular cartilage) and facilitated penetration of CMBs into the bone matrix (a precursor of the subchondral region) (Fig. 2 *A* and *B*). The dense cellular layer developed into cartilage and integrated with the bone matrix over 5 wk of cultivation (Fig. 2 *B* and *C*). Cells within early stage CMBs (1–5 d) were more penetrative and migratory than the cells in later stage CMBs (7 d), as measured by the cellular content of the subchondral region (Fig. 1*D*). Chondrogenic differentiation capabilities of fused CMB at different stages of maturity were similar, as indicated by the

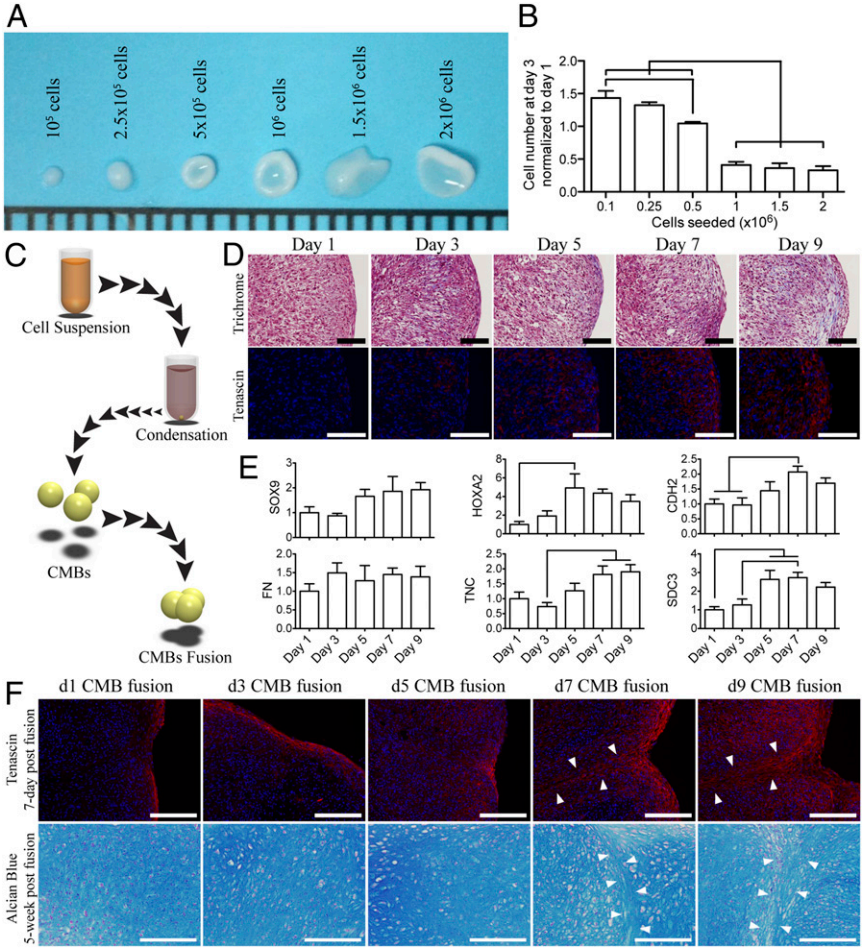

Fig. 1. Generation and fusion of CMBs formed in vitro. (*A*) Day-3 CMBs created from 1 $\times$ 10^5 to 2 $\times$ 10^6 hMSCs. (*B*) The DNA content in the condensed cellular body was quantified and normalized to the initial seeding DNA content. (*C*) Schematic of the condensation and fusion of CMBs. (*D*) At day 7, CMBs began to develop tangential cellular lining along the outer surface (*Upper Row*, Trichrome). The periphery surface of d7 and d9 CMBs stained for tenascin, an indication of boundary setting. (*E*) Boundary of CMBs was also characterized by high expression of *TNC* and *SDC3* genes, and increased expression of *HOXA2* and *CDH2* genes. *SOX9*, chondrogenesis factor, gradually increases as CMBs became more mature. Fibronectin expression, FN, remained constant. (*F*) Fusion of CMBs at different developmental stages. At days 7–9 postfusion, all CMBs showed tenascin deposition (*Upper Row*) at the periphery, in contrast to early stage CMBs (d1-5). Chondrogenesis in fused early stage CMBs resulted in a homogenous glycosaminoglycan structure (*Lower Row*), whereas the border between the adjacent CMBs was clearly seen in fused late stage CMBs (arrow). [Scale bars: (*A*) 1 mm; (*D*) 100 μm; and (*F*) 200 μm.] The lines in *B* and *E* indicate significant differences between the groups ($P < 0.05$).

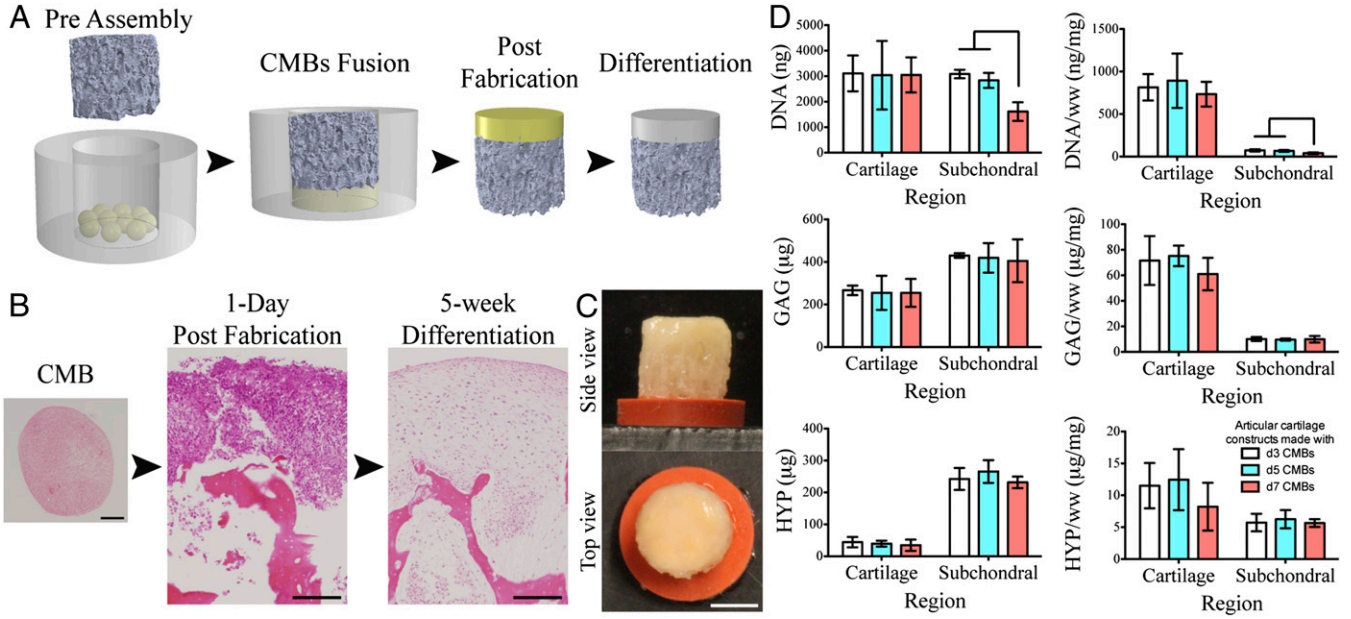

Fig. 2. Effect of the CMB developmental stage on cartilage formation. (*A*) To form articular cartilage on bone substrate, CMBs were placed into a PDMS ring, a bone scaffold was inserted and pressed onto CMBs to cause CMBs to fuse and penetrate inside the scaffold pores resulting in a composite osteochondral construct. After differentiation, the cellular layer formed into cartilage and integrated with the porous scaffold. (*B*) CMBs and osteochondral constructs at d1 and week 5 post fusion (H&E). Histological and immunohistochemical sections of the bioengineered cartilage and subchondral bone indicating appropriate matrix composition and cartilage formation. (*C*) Top and side views of the articular cartilage plug with the fused CMBs developed into thick cartilage layer covering the whole construct surface. (*D*) After 5 wk of chondrogenic induction, cartilage layers created from d3, d5, and d7 CMBs had similar contents of DNA, glycosaminoglycan (GAG), and hydroxyproline (HYP). Subchondral regions had similar GAG and HYP contents, and significantly lower DNA content for d7 CMBs, suggesting reduced migratory and integrative ability. [Scale bars: (*B*) 200 μm and (*C*) 2 mm.] Lines in *D* indicate significant differences between the groups ($P < 0.05$).

amounts of glycosaminoglycan and hydroxyproline (Fig. 1*D*). However, the resulting mechanical properties of the articular cartilage tissues were significantly different (Table 1). Young's modulus of cartilage was significantly higher for the early stage CMBs than the late stage CMBs. The corresponding friction coefficients appeared different, but not significantly. Notably, the Young's modulus (>800 kPa, Table 1) and equilibrium friction coefficient (~0.28, Table 1 and Fig. S1) of cartilage engineered from early stage CMBs over 5 wk in vitro were in the psyiological ranges for adult human articular cartilage.

Anatomically Shaped Cartilage Grown in Vitro. The condylar cartilage was engineered by press-molding CMBs onto anatomically shaped porous bone scaffolds (Fig. 3*A* and Movie S1). The CMBs formed a dense cellular layer penetrating into the scaffold and developed into a thick cartilage layer (>1 mm) covering the condylar surface of the scaffold after 5 wk of cultivation (Fig. 3*B*). Histological analysis revealed physiologic-like articular cartilage tissue structure (Fig. 3 *C*–*Z*). The cartilaginous ECM contained high amounts of glycosaminoglycan and collagen type II (Fig. 3 *G*–*N*). In the deep zone (Fig. 3 *E*, *I*, *M*, *Q*, *U*, and *Y*), cells were found in lacunae surrounded by ECM rich in glycosaminoglycan (Fig. 3*I*) and collagen type II (Fig. 3*M*). The superficial zone (Fig. 3 *D*, *H*, *L*, *P*, *T*, and *X*) consisted of flat cells and lubricin-rich ECM arranged tangentially to the articular surface (Fig. 3*P*). In the subchondral region, ECM was composed of glycosaminoglycan, collagen type I, and collagen type X (Fig. 3 *F*, *J*, *N*, *R*, *V*, and *Z*).

Cartilage Repair by CMBs in an in Vitro Model. Using an in vitro model of cartilage defect similar to those used before (25), we evaluated the capacity of CMBs for cartilage regeneration. The fused CMBs completely filled the cartilage defect and integrated with the surrounding cartilage after 5 wk of cultivation under chondrogenic conditions. The integration strength was determined by the force and stress required to break the integration interface between the fused CMBs and the surrounding cartilage (26). Both the force and the stress were two orders of magnitude higher in the CMB group than in untreated control defects (2.5 ± 0.48 N vs. 0.03 ± 0.02 N; 399 ± 56 kPa vs. 4.4 ± 1.9 kPa, respectively) (Fig. 4*B*). The high integration strength correlated to the formation of cartilaginous ECM by fused CMBs (Fig. 4 *C* and *D*).

Discussion

Engineering of biological substitutes of tissues or even organs is becoming increasingly plausible but is still facing major hurdles. Cartilage has been a major focus of the field of tissue

Table 1. Mechanical properties of human cartilage engineered by CMB fusion

Articular cartilage constructs	Young's modulus, kPa	Minimum friction coefficient, μ_{min}	Equilibrium friction coefficient, μ_{max}
Day 3 CMBs	788 ± 200	0.049 ± 0.008	0.276 ± 0.033
Day 5 CMBs	825 ± 197	0.046 ± 0.010	0.283 ± 0.042
Day 7 CMBs	457 ± 46*	0.064 ± 0.013	0.334 ± 0.053

*Statistically different from the other groups ($P < 0.05$).

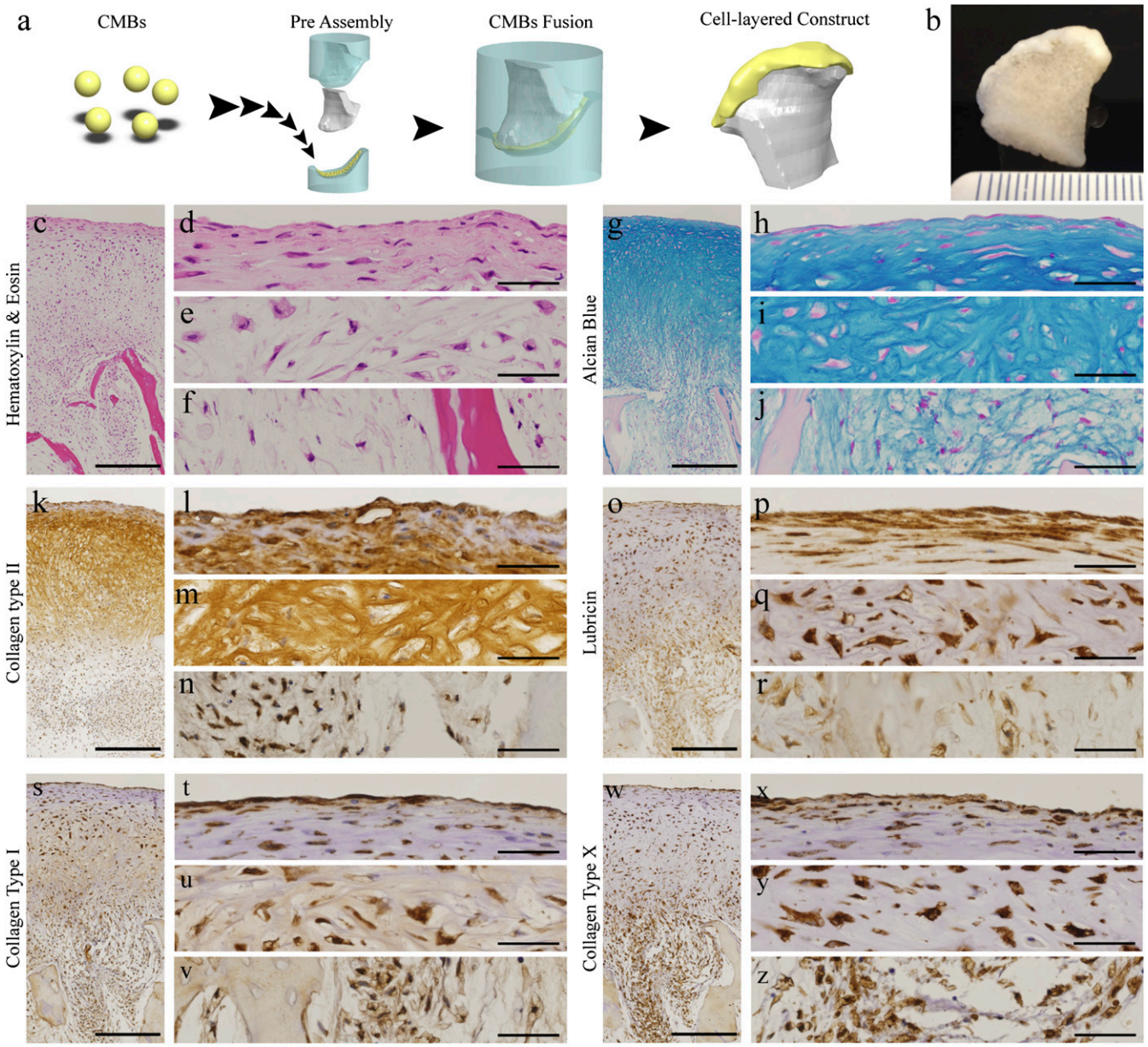

Fig. 3. The utility of CMB fusion for engineering large, anatomically shaped cartilage (*A*) CMBs were placed on the cartilage side of a mold in the exact shape of the condyle, an anatomically shaped porous scaffold was placed on the other side, and the two-piece mold was press-fit. CMBs fused together and adhered to the scaffold as a thick cellular layer along the articular surface. (*B*) Anatomical layer of articular cartilage on underlying bone after 5 wk of cultivation. (*C–Z*) Histological and immunohistochemical analysis of cartilage matrix stained for (*C–F*) H&E, (*G–J*) Alcian blue for GAG, (*K–N*) anticollagen type II, (*O–R*) antilubricin, (*S–V*) anticollagen type I, and (*W–Z*) anticollagen type X. (*C*, *G*, *K*, *O*, *S*, and *W*) Low-magnification images. (*D–F*, *H–J*, *L–N*, *P–R*, *T–V*, and *X–Z*) High magnification images. (Scale bar: 500 μm in low-magnification images and 50 μm in high-magnification images.)

engineering, as an avascular tissue containing only one cell type, initially considered to be an easy target. Cartilage repair by autologous chondrocytes harvested from a patient's knee and expanded in culture was devised in 1994 (27) and, shortly after, became the first FDA-approved cell-therapy product. A different source of cells, such as bone-marrow or adipose hMSCs, would be of high clinical interest, as it would avoid tissue harvest from the knee associated with morbidity and risk of arthritis. Thus, far, autologous and allogeneic hMSCs have been used in clinical trials as a source of trophic factors to induce cartilage regeneration (28). However, no current method can generate mechanically functional human cartilage starting from hMSCs. The compositions and mechanical properties of cartilage generated from hMSCs remain inferior to those achieved by chondrocytes (16).

The design of tissue engineering systems is being increasingly guided by biological principles prompting the need to provide native-like ("biomimetic") environments to unlock the full biological potential of the repair cells. We hypothesized that the recapitulation of some aspects of mesenchymal condensation could lead to the formation of functional cartilage from hMSCs. We investigated the hMSC condensation and boundary setting in vitro (Fig. 1) to engineer cartilage by mimicking the physiologic milieu of early development. We showed that hMSCs underwent condensation into CMBs within 1 d, with boundaries setting as early as 7 d postaggregation.

Developmental studies showed that tenascin-C and syndecan-3, key boundary setting proteins during mesenchymal condensation, are highly expressed at the periphery of the developing

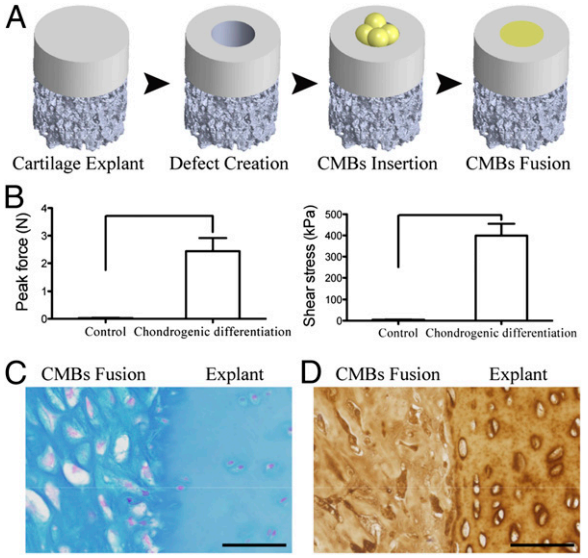

Fig. 4. Utility of CMBs for cartilage repair. (*A*) Cartilage defects (1.5 mm diameter) were created by biopsy punch and filled with pressed CMBs to fuse and fill the defect. (*B*) After 5 wk of chondrogenic induction, CMBs formed cartilage tissue that integrated with the native cartilage, as evidenced by the measured peak force and shear stress needed to break the integration surface. The high integration strength was due to the structural integration of glycosaminoglycan and collagen type II as indicated by (*C*) Alcian blue and (*D*) anticollagen type II immunohistochemistry stain. Lines in *B* indicate significant differences between the groups ($P < 0.05$). (Scale bar: 50 μm.)

chick limb outlining humerus, radius, and ulna (19, 21, 29). We found that only early stage CMBs (<7 d), before the setting of a boundary, could be homogenously fused and induced into chondrogenic differentiation and the formation of large and functional cartilage tissues. These findings are consistent with the reported role of tenascin-C in modulating cell attachment to fibronectin (30, 31).

In a previous study, osteochondral grafts were generated by a sequential 10-wk culture of chondrogenic and osteogenic hMSCs in a polymer scaffold. The compositions and mechanical properties of cultured tissues improved over time but remained subnormal (32). Whereas cartilage engineered from primary chondrocytes has successfully established physiologic mechanical property (15, 33), the highest compressive moduli reported for cartilage engineered from hMSCs was only ∼50% of normal (32). In the present study, large cartilaginous tissues with physiologic compressive modulus and lubricative property were successfully engineered in vitro by fusing CMBs and inducing their chondrogenic differentiation while also establishing an interface with subchondral bone (Fig. 2).

Unlike previously proposed scaffold-based or self-aggregating techniques for cartilage tissue engineering, the current method mimics mesenchymal condensation in tightly packed cellular aggregates that eventually develop into well-stratified cartilage interfaced with underlying bone. Remarkably, the compressive modulus and friction coefficient measured for engineered cartilage after 5 wk of cultivation were within the range of values measured for native articular cartilage (33, 34). Although the total collagen content was lower than the native cartilage, the resulting compressive modulus was associated with the high density of GAG (Fig. 2), similarly to the results previously reported with engineered cartilage from chondrocytes (15, 33). The fusion of CMBs before the setting of condensation boundaries was essential for the formation of functional cartilage constructs and their seamless integration with the underlying bone. Such biological fidelity has not been accomplished thus far by any method of cartilage formation from hMSCs.

By using the free-forming property of early stage CMBs, we engineered a continuous 1-mm thick cartilage layer covering the condylar surface of anatomical decellularized bone scaffold, with a composition, structure, and mechanical and surface properties resembling native articular cartilage (Fig. 3). The stratified formation of superficial surface with its lubricin-rich layer (Fig. 3 *O–R*) was associated with a physiologically low friction coefficient of the cartilaginous surface (Table 1). Furthermore, the presence of collagen type X at the interface between the cartilage layer and the subchondral region (Fig. 3 *W–Z*) suggested the development of calcified cartilage (35). GAG density near the bone interface within large constructs was lower than in the native cartilage–bone interface, which is rich in both collagen type X and GAG (36), suggesting the need for differentiation toward a more hypertrophic chondrocyte lineage or a longer culture time (37). Further studies will also need to confirm that the cartilage based on CMBs remains patent if challenged by in vitro hypertrophic regimens and following implantation into a joint.

The utility of fusing CMBs was further examined using an in vitro cartilage-defect model (Fig. 4). Following chondrogenic induction, the fused CMBs filled the defect and mechanically and structurally integrated with the surrounding native cartilage. This ability for integration holds promise that CMBs could be clinically applied to repair defects by simple injection delivery similarly to the chondrospheres system (38). Further studies will need to determine if the native joint environment would be sufficient to drive fused CMBs to undergo further chondrogenesis or if codelivery of other factors such as TGF-β will be required. An important component of clinical translation of this method will be the demonstration of engineered cartilage properties for hMSCs from numerous donors to assess the effects of age, sex, and systemic conditions (such as arthritis or diabetes) on tissue outcomes.

In summary, we report that mechanically functional human cartilage interfaced with subchondral bone substrate can be grown in vitro by mimicking some aspects of the pivotal developmental process of mesenchymal condensation. We demonstrate that this simple and effective technique results in clinically sized and anatomically shaped human cartilage with physiological stratification, Young's moduli (>800 kPA), and friction coefficients (<0.3). We further demonstrate that the same technique has potential use for repairing defects in native articular cartilage, as evidenced by the formation of cartilage–cartilage interface with integration strengths of 400 kPa. Conceivably, the same technique could be extended to bioengineer other tissues (39), such as tendon or meniscus, and to the use of other cell sources, such as embryonic and induced pluripotent stem cells (40, 41).

Materials and Methods

Please see *SI Materials and Methods* for hMSCs preparation, gene expression analysis, histology and immunohistochemistry, biochemical analysis, mechanical testing, and statistical analysis.

Generation and Fusion of CMBs. To generate CMBs, hMSCs were suspended in chondrogenic medium (high glucose DMEM supplemented with 10 ng/mL TGF-β_3, 100 nM dexamethasone, 50 μg/mL ascorbic acid-2-phosphate, 100 μg/mL sodium pyruvate, 40 μg/mL proline, 1% insulin, transferrin, sodium selenite (ITS) + mix, and 1% penicillin–streptomycin). To determine the optimal size of CMBs, hMSCs were suspended at the concentrations of 10^5, 2.5×10^5, 5×10^5, 10^6, 1.5×10^6, and 2×10^6 cells/mL. One milliliter of cell suspension was aliquoted into deep round-bottom 96-well plates (NUNC; Sigma-Aldrich) and centrifuged at $250 \times g$ for 5 min (Fig. 1*C*). Cells were incubated in a controlled humidified chamber [37 °C, 5% (vol/vol) CO_2] and culture media were replaced daily up to day 3. Samples were imaged and collected to analyze for DNA content ($n = 4$). CMBs formed by using 2.5×10^5 cells were used in all experiments due to their condensability and the formation of compact spherical CMBs. To investigate the development and maturity of the CMBs, they were incubated in culture medium and collected every other day starting at day 1 postcentrifugation up to 9 d. The CMBs were fixed in 10% (vol/vol) formalin for histological and immunohistochemical analysis or stored in TRIzol ($n = 4$) for gene expression analysis. To test the fusion capability of CMBs, three CMBs were pressed with a stainless steel block inside a polydimethylsiloxane (PDMS) wells (3 mm in diameter and 2 mm deep) at

days 1, 3, 5, 7, and 9 postcentrifugation (Fig. 1*C*), cultured for up to 5 wk, and evaluated histologically.

Generation of Cylindrical Cartilage Plugs. Eight CMBs (day 3, 5, or 7) were placed inside a PDMS ring (4 mm inner diameter × 4.5 mm high). Decellularized cylindrical trabecular bone matrix scaffolds (4 mm diameter × 4 mm high) were processed as previously described (42) and pressed inside the ring on the top of CMBs. Osteochondral constructs were formed by pressing the bone portion into the CMB layer. The internal geometry of the mold, with 0.5 mm of free space for the formation of the cartilage layer, maintained consistency of the applied pressure from one sample to another. A cartilage layer could be formed reproducibly by pressing the CMB layer onto a stainless steel block, but not by spontaneous fusion of CMBs without applying pressure. The constructs were cultured for 5 wk and analyzed mechanically ($n = 4$), biochemically ($n = 4$), and histologically ($n = 4$).

Generation of Anatomically Shaped Cartilage. A 3D image of an anatomical human condyle was obtained from a CT scan of a patient as in our previous studies (43). A 1-mm thick cartilage region was designed from the reconstructed 3D image to cover the articular surface of the condyle. As for the osteochondral plugs described above, anatomically shaped constructs were formed by pressing the bone portion into the CMB layer, by using a mold providing 1 mm of free space for the formation of the cartilage layer. A PDMS mold was created and cut into two pieces: one to hold the scaffold and the other to contain the articular cartilage side for pressed molding of CMBs (Fig. 3*A* and Movie S1). A total of 120 CMBs (day 3) were placed inside the mold at the articular cartilage side. Anatomical human condyle scaffolds created from decellularized trabecular bone, as previously described (43), were fitted inside the PDMS mold and lowered onto the articular cartilage side of the PDMS mold to fuse the CMBs and mold them into anatomical shape with cell penetration into the scaffold. The constructs were cultured for 5 wk with medium change twice per week.

Cartilage Defect Model. Osteochondral explants were cored from carpometacarpal joints of 2- to 4-mo-old cows, and cut into cylinders (4 mm in diameter × 4–6 mm thick) (44). The cartilage-defect model was created by removing a piece of cartilage at the center of the explant with a 1.5-mm biopsy punch creating a cartilage ring while leaving subchondral bone intact. Four CMBs were placed inside the void cartilage space and packed by pressing with a flat stainless steel block (Fig. 4*A*). The constructs were cultured in chondrogenic media or expansion media (negative control) for 5 wk and analyzed mechanically ($n = 4$) and histologically ($n = 4$).

ACKNOWLEDGMENTS. We gratefully acknowledge funding support of this work by the National Institutes of Health Grants DE016525 and EB002520 (to G.V.-N.).

1. Langer RS, Vacanti JP (1999) Tissue engineering: The challenges ahead. *Sci Am* 280(4): 86–89.
2. Nakao K, et al. (2007) The development of a bioengineered organ germ method. *Nat Methods* 4(3):227–230.
3. Tew SR, Kwan AP, Hann A, Thomson BM, Archer CW (2000) The reactions of articular cartilage to experimental wounding: Role of apoptosis. *Arthritis Rheum* 43(1): 215–225.
4. Quinn TM, Allen RG, Schalet BJ, Perumbuli P, Hunziker EB (2001) Matrix and cell injury due to sub-impact loading of adult bovine articular cartilage explants: Effects of strain rate and peak stress. *J Orthop Res* 19(2):242–249.
5. Chen CT, Burton-Wurster N, Lust G, Bank RA, Tekoppele JM (1999) Compositional and metabolic changes in damaged cartilage are peak-stress, stress-rate, and loading-duration dependent. *J Orthop Res* 17(6):870–879.
6. Züger BJ, et al. (2001) Laser solder welding of articular cartilage: Tensile strength and chondrocyte viability. *Lasers Surg Med* 28(5):427–434.
7. O'Driscoll SW, Keeley FW, Salter RB (1986) The chondrogenic potential of free autogenous periosteal grafts for biological resurfacing of major full-thickness defects in joint surfaces under the influence of continuous passive motion. An experimental investigation in the rabbit. *J Bone Joint Surg Am* 68(7):1017–1035.
8. Hangody L, Kish G, Kárpáti Z, Szerb I, Udvarhelyi I (1997) Arthroscopic autogenous osteochondral mosaicplasty for the treatment of femoral condylar articular defects. A preliminary report. *Knee Surg Sports Traumatol Arthrosc* 5(4):262–267.
9. Brittberg M, Nilsson A, Lindahl A, Ohlsson C, Peterson L (1996) Rabbit articular cartilage defects treated with autologous cultured chondrocytes. *Clin Orthop Relat Res* (326):270–283.
10. Vunjak-Novakovic G, et al. (1999) Bioreactor cultivation conditions modulate the composition and mechanical properties of tissue-engineered cartilage. *J Orthop Res* 17(1):130–138.
11. Pazzano D, et al. (2000) Comparison of chondrogensis in static and perfused bioreactor culture. *Biotechnol Prog* 16(5):893–896.
12. Mauck RL, et al. (2000) Functional tissue engineering of articular cartilage through dynamic loading of chondrocyte-seeded agarose gels. *J Biomech Eng* 122(3):252–260.
13. Lima EG, et al. (2004) Functional tissue engineering of chondral and osteochondral constructs. *Biorheology* 41(3-4):577–590.
14. Hu JC, Athanasiou KA (2006) A self-assembling process in articular cartilage tissue engineering. *Tissue Eng* 12(4):969–979.
15. Lima EG, et al. (2007) The beneficial effect of delayed compressive loading on tissue-engineered cartilage constructs cultured with TGF-beta3. *Osteoarthritis Cartilage* 15(9):1025–1033.
16. Mauck RL, Yuan X, Tuan RS (2006) Chondrogenic differentiation and functional maturation of bovine mesenchymal stem cells in long-term agarose culture. *Osteoarthritis Cartilage* 14(2):179–189.
17. Mackay AM, et al. (1998) Chondrogenic differentiation of cultured human mesenchymal stem cells from marrow. *Tissue Eng* 4(4):415–428.
18. Murdoch AD, et al. (2007) Chondrogenic differentiation of human bone marrow stem cells in transwell cultures: Generation of scaffold-free cartilage. *Stem Cells* 25(11): 2786–2796.
19. Hall BK, Miyake T (2000) All for one and one for all: Condensations and the initiation of skeletal development. *Bioessays* 22(2):138–147.
20. DeLise AM, Fischer L, Tuan RS (2000) Cellular interactions and signaling in cartilage development. *Osteoarthritis Cartilage* 8(5):309–334.
21. Mackie EJ, Murphy LI (1998) The role of tenascin-C and related glycoproteins in early chondrogenesis. *Microsc Res Tech* 43(2):102–110.
22. Mackie EJ, Thesleff I, Chiquet-Ehrismann R (1987) Tenascin is associated with chondrogenic and osteogenic differentiation in vivo and promotes chondrogenesis in vitro. *J Cell Biol* 105(6 Pt 1):2569–2579.
23. Sekiya I, Vuoristo JT, Larson BL, Prockop DJ (2002) In vitro cartilage formation by human adult stem cells from bone marrow stroma defines the sequence of cellular and molecular events during chondrogenesis. *Proc Natl Acad Sci USA* 99(7): 4397–4402.
24. Tuli R, et al. (2003) Transforming growth factor-beta-mediated chondrogenesis of human mesenchymal progenitor cells involves N-cadherin and mitogen-activated protein kinase and Wnt signaling cross-talk. *J Biol Chem* 278(42):41227–41236.
25. Pretzel D, et al. (2013) A novel in vitro bovine cartilage punch model for assessing the regeneration of focal cartilage defects with biocompatible bacterial nanocellulose. *Arthritis Res Ther* 15(3):R59.
26. Obradovic B, et al. (2001) Integration of engineered cartilage. *J Orthop Res* 19(6): 1089–1097.
27. Brittberg M, et al. (1994) Treatment of deep cartilage defects in the knee with autologous chondrocyte transplantation. *N Engl J Med* 331(14):889–895.
28. Mastbergen SC, Saris DB, Lafeber FP (2013) Functional articular cartilage repair: Here, near, or is the best approach not yet clear? *Nat Rev Rheumatol* 9(5):277–290.
29. Koyama E, Leatherman JL, Shimazu A, Nah HD, Pacifici M (1995) Syndecan-3, tenascin-C, and the development of cartilaginous skeletal elements and joints in chick limbs. *Dev Dyn* 203(2):152–162.
30. Chiquet-Ehrismann R, Kalla P, Pearson CA, Beck K, Chiquet M (1988) Tenascin interferes with fibronectin action. *Cell* 53(3):383–390.
31. Hsia HC, Schwarzbauer JE (2005) Meet the tenascins: multifunctional and mysterious. *J Biol Chem* 280(29):26641–26644.
32. Tuli R, et al. (2004) Human mesenchymal progenitor cell-based tissue engineering of a single-unit osteochondral construct. *Tissue Eng* 10(7-8):1169–1179.
33. Freed LE, Langer R, Martin I, Pellis NR, Vunjak-Novakovic G (1997) Tissue engineering of cartilage in space. *Proc Natl Acad Sci USA* 94(25):13885–13890.
34. Carter MJ, Basalo IM, Ateshian GA (2007) The temporal response of the friction coefficient of articular cartilage depends on the contact area. *J Biomech* 40(14): 3257–3260.
35. Eyre D (2002) Collagen of articular cartilage. *Arthritis Res* 4(1):30–35.
36. Pacifici M (1995) Tenascin-C and the development of articular cartilage. *Matrix Biol* 14(9):689–698.
37. Scotti C, et al. (2010) Recapitulation of endochondral bone formation using human adult mesenchymal stem cells as a paradigm for developmental engineering. *Proc Natl Acad Sci USA* 107(16):7251–7256.
38. Schubert T, et al. (2009) Long-term effects of chondrospheres on cartilage lesions in an autologous chondrocyte implantation model as investigated in the SCID mouse model. *Int J Mol Med* 23(4):455–460.
39. Arthur A, Zannettino A, Gronthos S (2009) The therapeutic applications of multipotential mesenchymal/stromal stem cells in skeletal tissue repair. *J Cell Physiol* 218(2): 237–245.
40. Oldershaw RA, et al. (2010) Directed differentiation of human embryonic stem cells toward chondrocytes. *Nat Biotechnol* 28(11):1187–1194.
41. Teramura T, et al. (2010) Induction of mesenchymal progenitor cells with chondrogenic property from mouse-induced pluripotent stem cells. *Cell Reprogramming* 12(3):249–261.
42. Grayson WL, et al. (2008) Effects of initial seeding density and fluid perfusion rate on formation of tissue-engineered bone. *Tissue Eng Part A* 14(11):1809–1820.
43. Grayson WL, et al. (2010) Engineering anatomically shaped human bone grafts. *Proc Natl Acad Sci USA* 107(8):3299–3304.
44. Tognana E, et al. (2005) Adjacent tissues (cartilage, bone) affect the functional integration of engineered calf cartilage in vitro. *Osteoarthritis Cartilage* 13(2):129–138.